Multi-Echo Gradient-Echo Spin-Echo with Echo-Planar Imaging for simultaneous quantification of T2* and T2

Joana Rita Mayer Rodrigues Vera-Cruz

Supervisors:
Prof. Sebastian Weingärtner
Prof. Rita Gouveia Nunes

Instituto Superior Técnico, Lisboa, Portugal

July 2022

Abstract

Motivation: T_2* and T_2 contrast-based sequences provide complementary information for MR applications. The Gradient-Echo and Spin-Echo (GESE) sequence has been developed to facilitate the simultaneous acquisition of T_2* and T_2-weighted images.
Objective: Corroborate the results reported in existing studies that tested the GESE sequence with EPI readout in the myocardium, WM and GM.
Methods: The GESE sequence was implemented through pulse programming by modifying the standard implementation of the ME-GE with EPI readout. Two variations tested - with simple and with composite refocusing pulses. Phantom scans and in-vivo scans of two healthy volunteers were conducted. Subsequently, a pixel-wise least squares fit was performed for computing quantitative T_2* and T_2 maps, from which ROIs were defined and mean values were extracted.
Results: Results obtained with simple and composite refocusing pulses, were respectively: for WM T_2*: (55 ± 1 ; 52 ± 2) ms , T_2: (64 ± 2 ; 64 ± 4) ms , for GM (T_2*: 57 ± 2 ; 56 ± 3) ms , T_2: (78 ± 5; 80 ± 8) ms and for Myocardium T_2*: (25 ± 10 , 27 ± 12) ms; T_2: (34 ± 14, 46 ± 32) ms.
Conclusions: The values of T_2* and T_2 using the GESE sequence with composite pulse, for the myocardium and WM were similar to the ones reported in literature and generated relative errors between 1.6 and 6.1%. For GM, both values were more distant from to the ones reported in literature, with relative errors of 12.0% and 12.7%.

Keywords: Gradient-Echo Spin-Echo, EPI readout, T_2* mapping, T_2 mapping, Quantitative MRI;

1. Introduction

Gradient-Echo (GE) T_2*-weighted sequences are widely used in several Magnetic Resonance (MR) applications such has Susceptibility-Weighted (SW) imaging, Perfusion Weighted Imaging (PWI) and Functional Magnetic Resonance Imaging (fMRI) [7]. There are two types of magnetic inhomogeneities that lead to faster T_2* decay: macroscopic inhomogeneities and microscopic inhomogeneities. Macroscopic inhomogeneities are constant within voxels and can be caused by air-tissue boundaries, metallic implants, or deoxyhemoglobin in small veins. Microscopic inhomogeneities change within a voxel and can arise from blood products, iron deposits, or paramagnetic contrast agents.

Besides its wide range of clinical applications, GE sequences provide more advantages, such as short acquisition times through the use of short Echo Time (TE)s and valuable data for Quantitative Magnetic Resonance Imaging (qMRI) and more precise physiological and pathological evaluation of tissues and organs [15]. However, there are some limitations associated with GE sequences, such as low inherent Signal to Noise Ratio (SNR) due to the use of low Flip Angle (FA)s and higher sensitivity to B_0 inhomogeneities.

T_2 contrast-based sequences can help assess the pathological status of the tissues, as it has been proven that the T_2 relaxation times vary between healthy and pathological tissues [5]. An example of an MR application where T_2-based sequences are widely used is Cardiovascular Magnetic Resonance Imaging (CMR). Myocardial tissues with a high water content have higher T_2 relaxation times (slower relaxation times) and therefore appear brighter in the images. As is known for myocardial tissues and other tissues, edema

is highly associated with acute injury. T_2-weighted sequences have also been useful for the pathological assessment of other anatomical regions, such as the brain, kidneys, and lungs.

It has been proven that T_2* and T_2 contrast-based sequences provide complementary information on MR applications such as Perfusion Susceptibility Imaging and CMR [12]. In Perfusion Susceptibility Imaging, T_2*-based sequences provide relatively high Contrast to Noise Ratio (CNR) and sensitivity to macro vasculature diameters whereas T_2*-based sequences provide lower sensitivity to contrast agent-induced signal changes but higher sensitivity to microvasculature changes. Therefore, the acquisition on both GE-PWI and Spin-Echo (SE)-PWI is often performed to improve diagnostic value [12]. Additionally, in CMR Blood Oxygenation Level-Dependent (BOLD) Magnetic Resonance Imaging (MRI) techniques can be used to assess myocardial oxygenation with no exogenous contrast agent. In this context, both T_2* and T_2 increase if there are higher concentrations of carbon dioxide in the blood that result in vasodilation. [6]. Hence, Gradient-Echo and Spin-Echo (GESE) sequence has been developed to facilitate the simultaneous acquisition of GE and SE [8, 10, 11, 13, 14, 16].

In summary, the GESE sequence, depicted in Figure 1, comprises the application of an excitation pulse, followed by two GE acquisitions and after the second acquisition a refocusing pulse is applied, followed by three mixed SE acquisitions. This sequence allows the simultaneous quantification of T_2* and T_2 through the data to the signal equation.

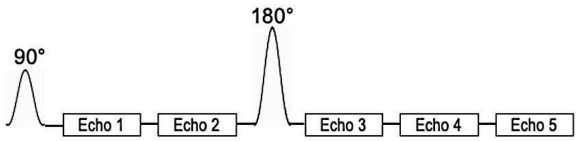

Figure 1: Sequence schematics of the GESE. The GESE acquires two GE echoes and three mixed SE echoes. Retrieved from [10].

To capture subtle Nuclear Magnetic Resonance (NMR) relaxation effects GESE has been implemented with Echo Planar Imaging (EPI) readout high temporal resolution. In order to reduce readout times and avoid geometric distortions due to T_2* dephasing, Parallel Imaging (PI) techniques, such as SENSitivity Encoding (SENSE), can be combined with EPI [13].

1.1. Objectives

Given that very few reports have so far been published regarding the use of the GESE-EPI sequence for BOLD MRI techniques, this work has as its principal objectives the expansion of the available body of literature and the corroboration of the results reported in existing studies that tested this sequence in the human brain and heart. In addition, this study aims to complement the previous development of GESE-EPI by its application in different a MRI scanner.

Moreover, at the beginning of this study an additional objective was set, which consisted of implementing the GESE sequence with spiral readout. However, given the time restriction, this objective was dropped.

2. Methodology

Since the GESE sequence is not provided by the scanner's vendor (Philips), it was implemented through pulse programming by modifying the standard implementation of the multi-echo Fast-Field Echo (FFE) with EPI readout.

The FFE sequence consisted of a 90° excitation pulse with sinc profile, five-echo single-shot EPI readouts, and a Spectral Presaturation with Inversion Recovery (SPIR) fat suppression pulse.

The modifications performed in the product implementation included the addition of a refocusing pulse between the second and third echoes, three slice selection gradients, two phase-encoding gradients, and two frequency encoding gradients, which will be further explained below. All these added elements increased the duration of the sequence by seven milliseconds. Additionally, one phase encoding gradient was removed. For debugging purposes and to test different combinations of sequence elements, the implementation allows the user to selectively choose which elements to include. The final implementation of the GESE sequence is shown in Figure 2, in which all modifications performed are colored.

2.1. Image Acquisition

All scans acquired were performed on a 3.0T scanner (Ingenia, Philips, Best, The Netherlands)

2.1.1 Phantom

Phantom imaging was performed using the International Society for Magnetic Resonance in Medicine (ISMRM)/National Institute of Standards and Technology (NIST) system phantom.

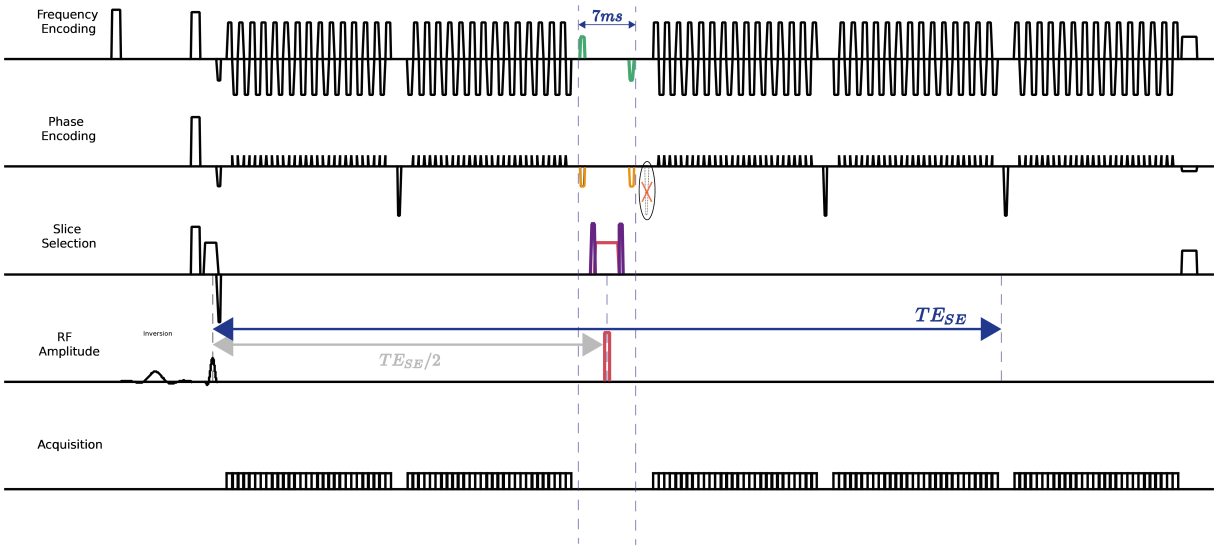

Figure 2: Sequence schematics of the five-echo GESE with EPI readout obtained through modifications performed to the standard implementation of the multi-echo FFE. The modifications include the addition of two frequency gradient blips (green), two phase gradient blips (yellow), two crusher gradients (purple), and a slice selection gradient and refocusing pulse (red). The yellow cross represents the removal of the first prephasing gradient along the phase encoding direction of the third echo acquisition. The added elements increased the sequence duration by 7 ms. The schematic was generated by the Philips' Graphical Viewer Environment (GVE).

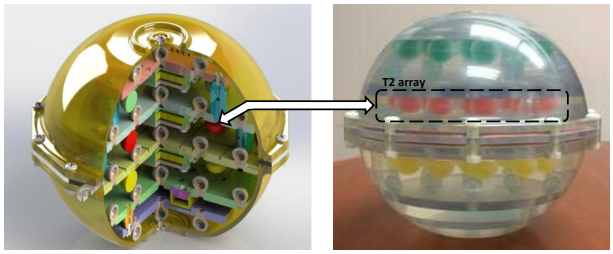

Figure 3: ISMRM/NIST system phantom composed of three layers with sphere arrays filled with different concentrations of $NiCl_2$, $MnCl_2$ and H_2O, resulting in different values of T_1, T_2 and proton density. For this study only the T_2 layer was used. Adapted from [2, 9]

Table 1: Imaging parameters used for the phantom experiments.

Imaging Parameters	GESE | FFE | SE	Ref. T_2*	Ref. T_2
Technique	-	FFE	SE
Nº of echoes	5	20	9
Fast Imaging mode	EPI	-	GRASE (Turbo Spin-Echo (TSE)+EPI)
Factor	EPI factor = 29	-	TSE factor = EPI factor = 9
Shot mode	single-shot	-	multi-shot
SENSE factor	3	3	-
TE [ms]	10	1.19	7.9
ΔTE [ms]	19.4	1.5	-
FA	90°	50°	90° | 180°
TR [ms]	10 000	600	1 000
Partial Fourier (Halfscan)	no	0.6	no

A 15 channel head coil was used for the phantom experiments. For all scans a single slice was selected with coronal orientation with the following imaging parameters: Field Of View (FOV) = 270 × 270 mm^2, in-plane resolution = 3 × 3 mm, and slice thickness = 4 mm. The TE for GESE, FFE, SE was set to the shortest value, of 10 ms, and Repetition Time (TR) was set to 10000 ms, to allow for recovery of the longitudinal magnetization. All sequences, with the exception of the T_2 Reference sequence, were tested with SPIR fat suppression pulse. Additional imaging parameters are specified in Table 1. The proposed GESE sequence was tested with 2 different refocusing pulses: a 180y simple pulse or a 90y240x90y composite pulse.

2.1.2 Brain

The 15 channel head coil used in the phantom scans was also used for the brain scans. The sequences tested on the human brain were the proposed 2D five-echo GESE, FFE and SE. Due to time constraints, no Reference T_2* or T_2 mapping sequences were acquired. A single-slice was in transverse orientation was selected with: FOV = 230 × 230 mm^2, in-plane resolution of 2 × 2 mm, and slice thickness = 3 mm, EPI factor = 39, SENSE factor = 3 and with a SPIR fat suppresion pulse. Additional acquisition parameters are shown in Table 2.

Table 2: Imaging parameters used for the brain experiments.

Imaging Parameters	GESE | FFE | SE
Fast Imaging mode	EPI
Shot mode	single-shot
Nº of echoes	5
TE [ms]	14 (GESE and FFE); 31 (SE)
ΔTE [ms]	27.4
FA	90°
TR [ms]	3 000
Halfscan	no

2.1.3 Heart

Cardiac scans were performed using a 16-channel anterior coil and a 12-channel posterior coil. For all scans, a single slice was selected in the short axis plane (see Figure 4).

The five-echo GESE, FFE, SE, as well as, the Reference T_2* sequence and T_2 mapping sequences were acquired with the acquisition parameters shown in Table 3. For GESE, FFE and SE, a Spectrally Selective Attenuated Inversion Recovery (SPAIR) fat supression pulse was selected. Additionally, for the Reference T_2* and T_2 mapping sequence, a black-blood prepulse was selected. All scans were set with a trigger delay of end diastole (903 ms) to minimize the cardiac motion.

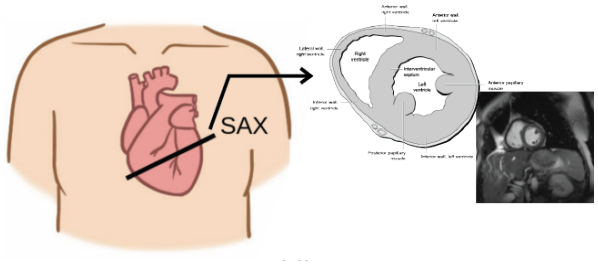

Figure 4: Short axis view of the heart with a clear depiction of the left and right ventricles. Adapted from [1, 3, 4]

2.2. Image Post Processing

All post-processing steps were carried out in Matlab R2021a using original scripts unless mentioned otherwise.

The reference T_2* and T_2 maps were generated inline by the scanner and the GESE T_2* and T_2 maps were computed offline using a 4-parameter [6] pixel-by-pixel least squares fit, as follows:

$$S(\tau) = \begin{cases} S_0^I \cdot e^{-\tau \cdot R_2^*} & , 0 < \tau < TE_{SE}/2 \\ S_0^{II} \cdot e^{TE_{SE} \cdot (R_2^* - R_2)} \cdot e^{-\tau \cdot (2 \cdot R_2 - R_2^*)} & , TE_{SE}/2 < \tau < TE_{SE} \end{cases} \quad (1)$$

where $S_0{}^I$ and $S_0{}^{II}$ are the equilibrium signals before and after the refocusing pulse, respectively, τ is the echo time and TE_{SE} is the time at which the spin-echo occurs.

For the phantom experiments, circular masks were created and mean T_2 and T_2^* values for each vial were computed. Correlation and Bland-Altman plots were performed using the values obtained with the proposed five-echo GESE and the proposed Reference sequence. For the in-vivo scans, individual masks were computed for each sequence presented, to avoid incorrect Region Of Interest (ROI) positioning due to volunteer motion. The left-ventricular (heart) and white- and gray-matter (brain) masks were manually drawn using an in-house developed MATLAB script.

3. Results

3.1. Phantom

Figure 5(a) and 5(b) contain the T_2* maps obtained with the reference and with the proposed GESE sequence, respectively. Figure 6(a) and 6(b) shows the T_2 maps computed using the reference and the proposed GESE sequence, respectively.

To assess the accuracy of T_2* and T_2 parameter estimation using the GESE sequence with composite pulse, T_2* (Figure 5(b)) and T_2 (Figure 6(b)) maps were computed and compared with scanner generated T_2* and T_2 maps acquired with standard vendor sequences used as reference, shown in Figures 5(a) and 6(a).

From the maps of the GESE, Reference T_2* and Reference T_2 sequences, mean values for T_2* and T_2 inside each of the fourteen ROIs were computed. The values obtained are represented in the format of correlation plots, in Figures 7(a) and 8(a), for ease of comparison. Some outlier points, that correspond to phantom spheres with higher values of T_2* and T_2, were excluded from this analysis, as they are not expected to be seen in-vivo. For outlier exclusion, a threshold of T_2* $>$ 100 ms and T_2 $>$ 200 ms was established. The variable "n" displayed in the correlation plots represents the number of ROIs taken into account.

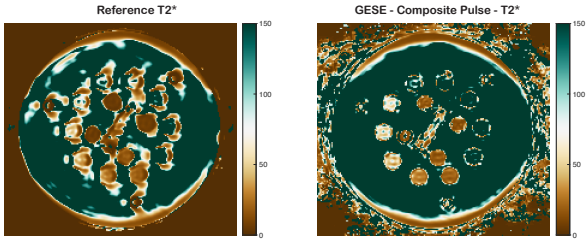

(a) (b)

Figure 5: T_2* maps computed from the **(a)** Reference T_2* sequence and **(b)** GESE with composite pulse sequence for the phantom.

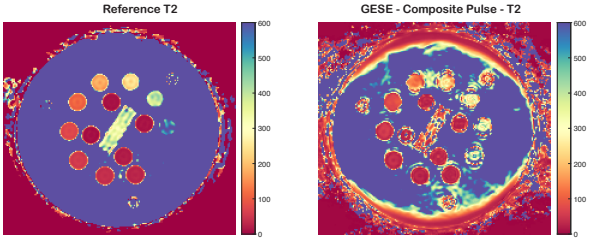

(a) (b)

Figure 6: T_2 maps computed from the **(a)** Reference T_2 sequence and **(b)** GESE with composite pulse sequence for the phantom.

Table 3: Imaging parameters used for the heart experiments.

Imaging Parameters	GESE | FFE | SE	T_2* ref	T_2 ref
Technique	-	FFE	SE
FOV $[mm^2]$	240 × 279	300 × 300	300 × 300
In-plane resolution $[mm]$	3.1 × 3.1	3.6 × 3.6	3.1 × 3.1
Slice thickness $[mm]$	8	10	8
Fast Imaging mode	EPI	Turbo Field Echo (TFE)	GRASE (TSE + EPI)
Factor	EPI factor = 31	8	TSE factor = 9 | EPI factor = 7
Shot mode	single-shot	multi-shot	multi-shot
Nº of echoes	5	15	9
TE [ms]	10	0.97	7.4
ΔTE [ms]	19.1	0.9	-
FA	90°	25°	90° | 180°
TR [ms]	1 200 (1 beat)	15	1 200 (1 beat)
SENSE factor	3	2	2

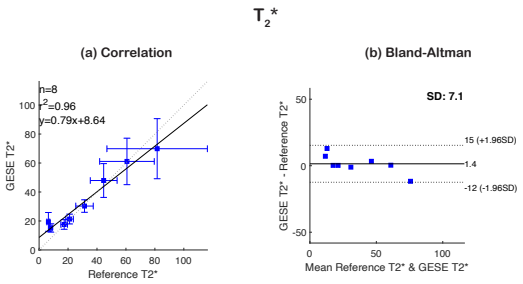

Figure 7: (a) Correlation and **(b)** Bland-Altman plots comparing the mean T_2* values obtained with the Reference T_2* and GESE with composite pulse sequences. Only nine out of the fourteen ROIs were considered.

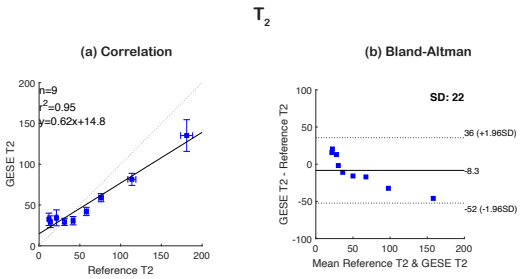

Figure 8: (a) Correlation and **(b)** Bland-Altman plots comparing the mean T_2 values obtained with the Reference T_2 and GESE with composite pulse sequences. Only thirteen out of the fourteen ROIs were considered.

3.2. Brain

For the analysis of the brain scans, two ROIs with circular shape were selected, white matter (ROI 1) and grey matter (ROI 2) regions. The ROIs are represented in Figure 9.

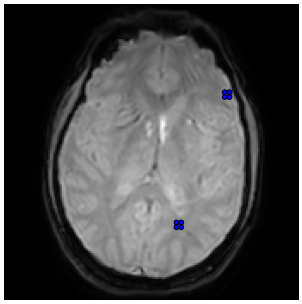

Figure 9: Representation of the two ROIs selected for analysis from the brain scans. One ROI corresponds to a grey matter region and the other corresponds to a white matter region.

T_2* and T_2 maps were computed from the scans obtained with the GESE sequence with both simple and composite pulses (for simplification, only the maps acquired with the composite pulse are shown, in Figures 10(a) and 10(b)), however, due to time restrictions, no reference T_2 and T_2^* mapping scans were acquired. Instead, the reported values will be compared against available literature. The mean values for T_2* and T_2 inside both ROIs are shown on Table 4, as well as the values extracted from the literature.

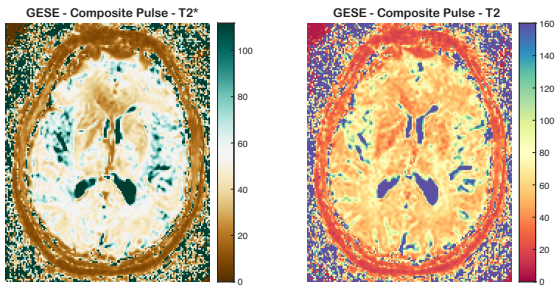

(a) (b)

Figure 10: In vivo brain **(a)** T_2* and **(b)** T_2 maps computed from the GESE with composite pulse sequence.

Table 4: Mean T_2* and T_2 values measured for the two brain ROIs using the GESE with either simple or composite pulse.

Sequence	Tissue	T_2* (ms) mean ± SD	T_2 (ms) mean ± SD
GESE - Simple Pulse	White matter (ROI 1)	55 ± 1	64 ± 2
	Gray matter (ROI 2)	57 ± 2	78 ± 5
GESE - Composite Pulse	White matter (ROI 1)	52 ± 2	64 ± 4
	Gray matter (ROI 2)	56 ± 3	80 ± 8

3.3. Heart

For the analysis of the cardiac scans, a single ROI was chosen within the myocardium, represented in Figure 11.

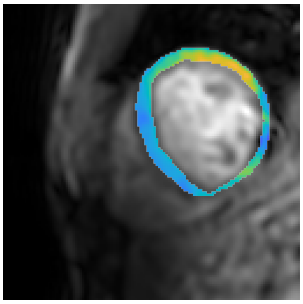

Figure 11: Representation of the ROI selected for analysis from the heart scans. The ROI corresponds to a region of the myocardium.

The T_2* and T_2 maps retrieved from the GESE with composite pulse and the reference sequences are shown in Figures 12 and 13 and the extracted mean ROI values are shown in Table 5.

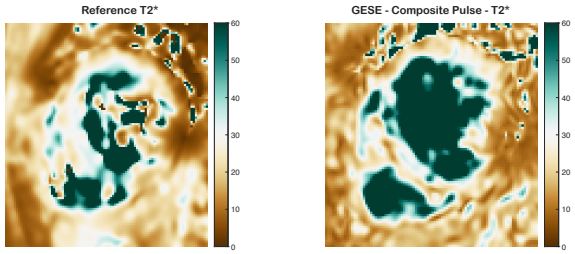

(a) (b)

Figure 12: T_2* maps computed from the **(a)** Reference T_2* sequence and **(b)** GESE with composite pulse sequence for the heart.

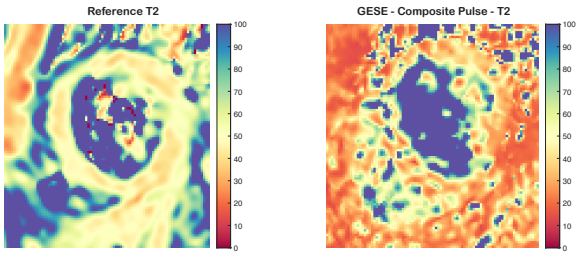

(a) (b)

Figure 13: T_2 maps computed from the **(a)** Reference T_2 sequence and **(b)** GESE with composite pulse sequence for the heart.

Table 5: Mean T_2* and T_2 values measured measured for the heart ROI using the GESE with either simple or composite pulse.

Sequence	T_2* (ms) mean ± SD	T_2 (ms) mean ± SD
Reference	24 ± 9	47 ± 7
GESE - Simple Pulse	25 ± 10	34 ± 14
GESE - Composite Pulse	27 ± 12	46 ± 32

4. Discussion

4.1. Phantom

The T_2* Correlation (Figure 7(a)) plot shows a correlation coefficient of 0.96, indicating a strong linear association between the T_2* obtained with GESE sequence and the T_2* obtained with Reference T_2* sequence. Five intermediate values, comprised roughly between a Reference T2* of 18 and 62 ms, are very close to the y=x equation (dashed line on the plot), which indicates strong proximity of values between both sequences. The Standard Deviation (SD) is visibly higher for the phantom spheres with higher values of T_2* which indicates that the measurements are less reliable for high T_2* values. Regarding the T_2* Bland-Altman (Figure 7(b)) plot, all values are inside the limits of agreement.

For T_2 even though there is a strong linear association between the T_2 values obtained with the GESE sequence and those obtained with the Reference sequence, as supported by the r^2 value of 0.95, this does not translate into the desired trend of having identical T_2 values for both sequences. The obtained linear equation's slope of 0.62 and offset of 14.8 shows that it differs significantly from the ideal linear equation, whose slope would be 1 and offset would be 0.

The less satisfactory results obtained for T_2 might be related to some limitations inherent to the GESE sequence. Since only 3 echoes with short echo spacing are used to estimate T_2, GESE sequence has limited capacity to estimate higher values of T_2.

4.2. Brain

After analysis of the results obtained for White matter (WM), it is possible to conclude that the GESE with composite pulse provided values of T_2* and T_2 were very similar to the values retrieved from literature using the same sequence, with relative errors of 6.1% and 1.6%, respectively. The values obtained deviated more from the literature values using other standard quantification sequences.

The values obtained for Gray matter (GM) generated higher relative errors when compared to literature using the same sequence. A possible cause might be related to inaccurate ROI position-

ing. However, the relative errors were reduced when compared to the values from literature using standard sequences.

4.3. Heart

After a more detailed inspection of the results obtained for the myocardium, it is possible to conclude that the GESE sequence with composite pulse provided values of T_2* and T_2 very similar to the values retrieved from literature using the same sequence, with relative errors of 1.8% and 6%, respectively.

5. Conclusions

Several limiting factors affected the results obtained, such as the reduced number of volunteers tested, which limits the comparison of the T_2* and T_2 values obtained with the GESE sequence versus the values retrieved from the literature. In addition, the limited number of echoes acquired limits the accuracy of the least-squares fit performed to obtain the quantitative maps. However, acquiring a higher number of echoes would compromise temporal resolution which could be a downside for applications where a temporal resolution is desired, such as CMR. Furthermore, the definition of ROIs was performed manually; therefore, a more robust technique should be used, such as automatic tissue segmentation, for a more precise selection of ROIs. In addition, because the TE_{SE} is not centered with any acquisition window, none of the echo images acquired is only T_2-weighted.

Further sequence optimization steps should be taken to improve the accuracy of T_2* and T_2 quantification using the developed sequence. First, TE_{SE} should be centered on the fifth acquisition window. This can be done by increasing the time interval between the second echo acquisition and the refocusing pulse. Second, different values of echo spacings (ΔTEs) should be tested for a wider range of tissue quantification. Lastly, the design of the crusher gradient pair and the slice selection gradient should be improved and more designs of composite pulses should be tested to fully mitigate the problems arising from the mismatch of the slice profile.

Further research steps include testing the sequence on the brain and heart in an increased number of volunteers for a more sustained comparison of the results obtained with the values retrieved from literature. Additionally, breath hold experiments should be conducted to further validate the use of the GESE sequence for BOLD CMR techniques.

Acronyms

NMR	Nuclear Magnetic Resonance
MRI	Magnetic Resonance Imaging
MR	Magnetic Resonance
FA	Flip Angle
BOLD	Blood Oxygenation Level-Dependent
SNR	Signal to Noise Ratio
CNR	Contrast to Noise Ratio
EPI	Echo Planar Imaging
GE	Gradient-Echo
FFE	Fast-Field Echo
TE	Echo Time
SE	Spin-Echo
GESE	Gradient-Echo and Spin-Echo
qMRI	Quantitative Magnetic Resonance Imaging
ISMRM	International Society for Magnetic Resonance in Medicine
NIST	National Institute of Standards and Technology
FOV	Field Of View
TR	Repetition Time
SENSE	SENSitivity Encoding
GVE	Graphical Viewer Environment
ROI	Region Of Interest
SD	Standard Deviation
SPIR	Spectral Presaturation with Inversion Recovery
SPAIR	Spectrally Selective Attenuated Inversion Recovery
TSE	Turbo Spin-Echo
TFE	Turbo Field Echo
SW	Susceptibility-Weighted
fMRI	Functional Magnetic Resonance Imaging
CMR	Cardiovascular Magnetic Resonance Imaging
PI	Parallel Imaging
PWI	Perfusion Weighted Imaging
WM	White matter
GM	Gray matter

References

[1] Heart normal short axis echo. https://pt.m.wikipedia.org/wiki/Ficheiro:Heart_normal_short_axis_echo.svg. Accessed: 2022-07-02.

[2] Magnetom Verio 3T. Accessed on November 10, 2021.

[3] Parasternal short axis view in the papillary plane. https://theory.labster.com/parasternal_short_axis_papillary_view/. Accessed: 2022-07-02.

[4] Short axis view. http://radiology.con.mk/cardiacmr/Anatomy/Short.html. Accessed: 2022-07-02.

[5] H. Abdel-Aty, O. Simonetti, and M. G. Friedrich. T2-weighted cardiovascular magnetic resonance imaging. *Journal of Magnetic Resonance Imaging*, 26(3):452–459, 2007.

[6] M. V. D. Boomen, M. K. Manhard, G. J. H. Snel, and S. Han. Blood Oxygen Level – Dependent MRI of the Myocardium. *Radiology*, 294(16):538–545, 2020.

[7] G. B. Chavhan, P. S. Babyn, B. Thomas, M. M. Shroff, and E. Mark Haacke. Principles, techniques, and applications of T2*-based MR imaging and its special applications. *Radiographics*, 29(5):1433–1449, 2009.

[8] S. Kaczmarz, F. Hyder, and C. Preibisch. Oxygen extraction fraction mapping with multi-parametric quantitative BOLD MRI: Reduced transverse relaxation bias using 3D-GraSE imaging. *NeuroImage*, 220(February):117095, 2020.

[9] K. E. Keenan, K. F. Stupic, M. A. Boss, and S. E. Russek. Comparison of T1 measurement using ISMRM/NIST system phantom., 2016. Accessed on November 10, 2021.

[10] M. K. Manhard, B. Bilgic, C. Liao, S. H. Han, T. Witzel, Y. F. Yen, and K. Setsompop. Accelerated whole-brain perfusion imaging using a simultaneous multislice spin-echo and gradient-echo sequence with joint virtual coil reconstruction. *Magnetic Resonance in Medicine*, 82(3):973–983, 2019.

[11] A. Prinster, C. Pierpaoli, R. Turner, and P. Jezzard. Simultaneous measurement of ΔR2 and ΔR2* in cat brain during hypoxia and hypercapnia. *NeuroImage*, 6(3):191–200, 1997.

[12] H. Schmiedeskamp, M. Straka, R. D. Newbould, G. Zaharchuk, B. Jalal, J.-m. Olivot, M. E. Moseley, and G. W. Albers. Combined Spin-And Gradient-Echo Perfusion-Weighted Imaging. *Magnetic Resonance in Medicine*, 68(1):30–40, 2012.

[13] J. T. Skinner, R. K. Robison, C. P. Elder, A. T. Newton, B. M. Damon, and C. C. Quarles. Evaluation of a multiple spin- and gradient-echo (SAGE) EPI acquisition with SENSE acceleration: Applications for perfusion imaging in and outside the brain. *Magnetic Resonance Imaging*, 32(10):1171–1180, 2014.

[14] A. M. Stokes, J. T. Skinner, T. Yankeelov, and C. C. Quarles. Assessment of a simplified spin and gradient echo (sSAGE) approach for human brain tumor perfusion imaging. *Magnetic Resonance Imaging*, 34(9):1248–1255, 2016.

[15] M. Y. Tang, T. W. Chen, X. M. Zhang, and X. H. Huang. GRE T2*-weighted MRI: Principles and clinical applications. *BioMed Research International*, 2014:312142, 2014.

[16] Y. Wang, R. Zhang, B. Zhang, C. Wang, H. Wang, X. Zhang, K. Zhao, M. Yang, X. Wang, and J. Zhang. Simultaneous R2, R2' and R2* measurement of skeletal muscle in a rabbit model of unilateral artery embolization. *Magnetic Resonance Imaging*, 61(May):149–157, 2019.